Secondary Electron Emission in Glow Discharge Plasmas

Keroshnar Pardnsar

Department of Physics, College of Science, University of Madras, Marina Campus, Chennai, INDIA

Abstract

In this study, the emission coefficient of secondary electrons for some common gas discharges employed in thin film deposition processes and techniques was determined as function of some affecting parameters. This coefficient may play negative role in the optimization of discharge plasma employed for practical uses and applications. Therefore, this coefficient is often minimized even though the experimental conditions are shifted from their optima in order to ensure that the consumption of supplied power is high as much as possible. This study was supported by experimental data from a reactive plasma sputtering system used for deposition of some metal oxide and nitride thin films.

1. Introduction

Today, plasma can be generated, controlled and employed in physics laboratories at reasonably low requirement, cost and risk conditions. Over 150 years ago, sputtering was observed for the first time by Grove when he was working on discharge plasma [1,2]. It was really interesting to control a process in which an atom is removed from a target, carried through plasma and deposited on a substrate [3 6]. When plasma is totally and precisely controlled, then the whole sputtering process is accordingly controlled [7 10].

The dc glow discharge has been historically important, both in applications of weakly ionized plasmas and in studying the properties of the plasma medium [11,12]. A dc discharge has one obvious feature, its macroscopic time independence, that is simpler than radiofrequency (rf) discharges. However, the need for the current, which provides the power for the discharge, to be continuous through the dc sheath provides an additional complication to the operation [13-15].

Glow discharge is low-temperature neutral plasma where the number of electrons is equal to the number of ions despite that local but negligible imbalances may exist at walls [7]. Glow discharge is described as self-sustaining plasma, i.e., the avalanche effect of electrons keeps the continuous production of ion species [16,17]. The avalanche condition from the initial applied voltage in a typical low-pressure discharge is shown in Fig. (1) [16].

If an initial voltage is applied on a gas sample between two electrodes at sufficient separation, little current will flow through this sample due to the ionization effects in the gas [18]. As the applied voltage is increased to reach the breakdown voltage, the energy given to ions is increased too that increases their collisions with atoms and electrodes. Accordingly, more ions and electrons are produced due to the ionization and secondary electron emission effects, which lead to increase the flowing current gradually approaching the breakdown point beyond which the avalanche occurs and the current increases drastically in the Townsend discharge region [19].

If an energetic ion approaches the surface of a solid (target), one or all of the following phenomena may occur:
• The ion may be reflected, being getting neutralized in the process.
• The collision of the ion may cause the target to eject an electron, called the secondary electron.
• The ion may become buried in the target.
• The ion collision might be responsible for some structural changes in the target material.
• The ion collision may set up a series of collisions between atoms of the target, leading to the ejection of one of the target atoms. This ejection process is known as sputtering [20].
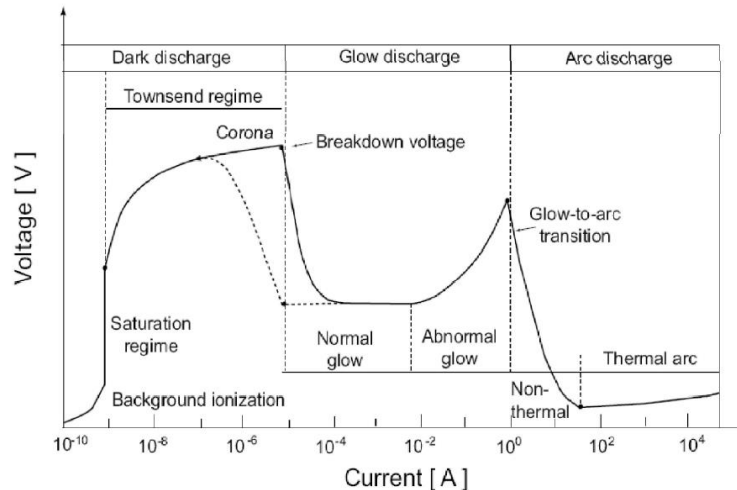
Fig. (1) Different regions of plasma discharge on the I-V characteristics [16]

Figure (2) summarizes all the phenomena mentioned above. The principles of sputtering can be understood using a simple momentum transfer model, which enables to visualize how atoms are ejected from a surface as a result of two collisions.

The series of collisions in the target, generated by the primary collision at the surface, is known as a collision cascade. It is a matter of probability whether this cascade leads to the sputter ejection of an atom from the surface (which will require at least two collisions) or the cascade heads off into the interior of the target, gradually dissipating the energy of the primary impact, ultimately to lattice vibration. Sputtering ejection is rather energy inefficient, with typically 1% of the incident energy reappearing as the energy of the sputtered atom. The rest of the energy is lost in the form of heating of the chamber walls, parts inside the chamber and the target [21].
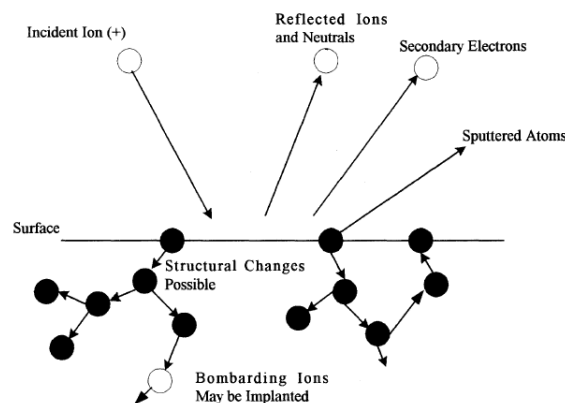

Fig. (2) Interaction of ions with surfaces [21]

Sputtering is complex process, which is highly dependent on number of process parameters, such as deposition pressure, discharge voltage, discharge current, target-to-substrate distance, gas compositions, process gas flow rate, reactive gas flow rate in case of reactive sputtering, substrate biasing, etc. [22-24].

The sputtering process is quantitatively described by the sputtering yield, which is defined as the number of target atoms ejected per incident particle. This yield depends on the target materials and their crystalline structure, the energy of incident particles, and the incidence angle of the bombarding particles [3,25]. When the mass of the bombarding particle is comparable or larger than that of the target atoms, the sputtering yield tends to be greatest. It is relatively independent of the target temperature and whether or not the bombarding species is ionized [25].

In the case where no bias is applied to the collection cylinder, both target and collection cylinder are at the same potential, the calculation of g is straight forward. The electrons are emitted in a cosine distribution with respect to the surface normal and the fraction of electrons that escape through the

hole for the ion beam, d_{esc}, is easily calculated. From this, $g=l/(l-d_{esc})$ can be determined [26]. With a bias on the collection cylinder, two questions must be answered: will electrons that used to escape now be collected? and will electrons that were collected now escape?

In order to answer those questions, the trajectories of emitted electrons was calculated. It was assumed that a constant electric field parallel to the target E_y was maintained (Fig. 3). The approximation of two parallel plates for the collection cylinder and target was found to be good by comparing this situation with the true set up of a flat target and a curved collection plate. The radius of curvature is large compared to the distance between the target and collection cylinder. Thus, the curvature is insignificant.
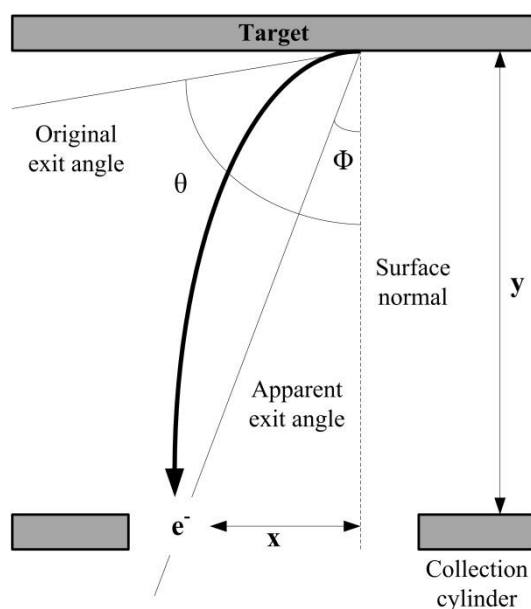

Fig. (3) Explanation of original and apparent exit paths of electron under the effect of electric field in discharge system

2. Modeling and Mathematical Treatment

The breakdown voltage is directly related to the pressure of the gas sample and the mean free path of secondary electrons. This relation between breakdown voltage (V_B) and gas pressure (p) is known as "Paschen's law" and given by [27]:

$$V_B = \frac{pdB}{log(pdA) - log\left(log\left(1 + \frac{1}{\gamma_e}\right)\right)} \qquad (1)$$

where A and B are constants and their values are determined by the properties of the used gas, as shown in Table (1), d is the inter-electrode distance (i.e., the distance between discharge electrodes), and $\square_e$ is the emission coefficient of the secondary electrons

The breakdown voltage (V_B) depends on the product ($p.d$), and weakly depends on the cathode material that defines the emission coefficient of secondary electrons [13]. As well, the breakdown voltage is proportional to the product $p.d$ at large values of this product and the electric field ($E=V/d$) is scaled linearly with the pressure [28].

In case of small values of the product $p.d$, only few collisions occur and higher voltage is applied to increase the probability of breakdown per collision. Hence, the minimum voltage required to ignite the discharge of a gas sample of pressure p over a distance d is defined at the minimum of Paschen's curve, as [19]

$$pd|_{V_{min}} = \frac{1}{A} log\left(1 + \frac{1}{\gamma_e}\right) \qquad (2)$$

If the pressure and/or inter-electrode distance is too large, ions generated in the gas are slowed by inelastic collisions, so that they strike the cathode with insufficient energy to produce secondary electrons. In most sputtering glow discharges, the discharge starting voltage is relatively high. Figure (4) shows the Paschen's curves of different gases. The electron mean free path (λ_e) is then related to the pressure by

 Printed in IRAQ

$$\lambda_e \cong p.d \qquad (3)$$

To initiate the discharge within the gas sample, the following condition must be satisfied [2]

$$p \geq \frac{\lambda_e}{d} \qquad (4)$$

According to the self-sustaining feature of glow discharge, the number of the produced electrons is just sufficient to produce the same number of ions to generate again the same number of electrons. These ions liberate electrons from the electrodes (secondary), atom-ion and ion-ion collisions. When this condition is satisfied, the voltage decreases and the current increases. This is said to be a "normal discharge".

Due to the recombination effects and excited atoms returning to ground state, the plasma begins to glow, as

$$A^* \rightarrow A + h\nu \qquad (4a)$$
$$A^+ + e^- \rightarrow A + h\nu \qquad (4b)$$

here A^* is an excited atom and e^- is a high-energy electron

Table (1) Typical values of A and B constants, E/p and ionization energy (V_i) for various gases [2]

Gas	A (Ion/pairs)/(cm.torr)	B V/(cm.torr)	E/p V/(cm.torr)	V_i (V)
H_2	5	130	150~600	15.4
He	3	34 / 25	20~150 / 3~10	24.5
N_2	12	342	100~600	15.5
Ar	14	180	100~600	15.7
O_2	-	-	-	12.2
Ne	4	100	100~400	21.5
Kr	17	240	100~1000	14
Xe	26	350	200~800	12.1
Hg	20	370	200~600	10.4
Air	15	365	100~800	-
CO_2	20	466	500~1000	13.7
H_2O	13	290	150~1000	12.6

Table (2) shows the values of secondary electron emission coefficients for three different metals when different ions are bombarding these targets.

Table (2) The secondary electron emission coefficients for three different metals when different ions are bombarding these targets [2]

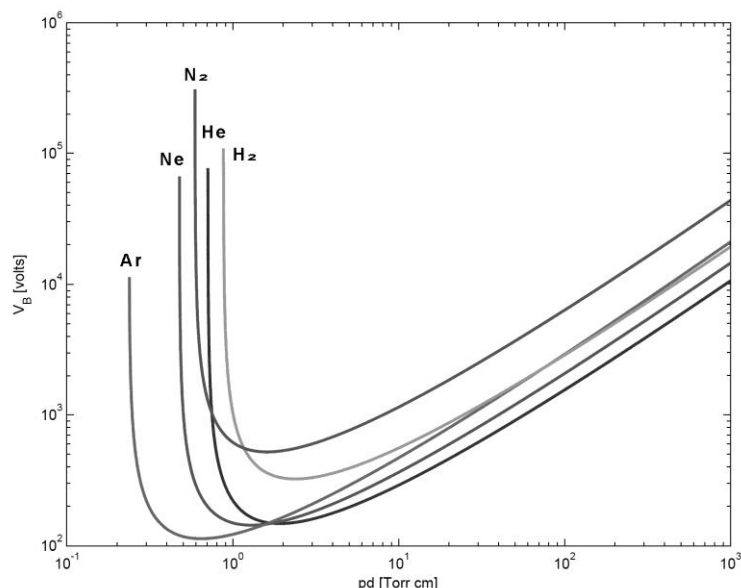| Target Material	Incident Ion	Ion Energy (eV) 200	600	1000
W	He^+	0.524	0.24	0.258
	Ne^+	0.258	0.25	0.25
	Ar^+	0.1	0.104	0.108
	Kr^+	0.05	0.054	0.108
	Xe^+	0.016	0.016	0.016
Mo	He^+	0.215	0.225	0.245
	He^{++}	0.715	0.77	0.78
Ni	He^+		0.6	0.84
	Ne^+			0.53
	Ar^+		0.09	0.156

Fig. (4) Paschen's curves of different common gases used in electric discharge applications [21]

3. Results and Discussion

Figure (5) shows the variation of secondary electron emission coefficient of cathode material with breakdown voltage of four different gases at pressure of 0.1 mtorr and inter-electrode distance of 4 cm. With such difference in the value of the emission coefficient (more than an order of magnitude), argon and nitrogen are highly preferred for using in discharge systems than hydrogen and helium. However, argon and nitrogen cannot replace helium in some applications of gas discharge, mainly gas lasers, as shown in Fig. (6). As well, hydrogen is the excellent choice for some other applications.
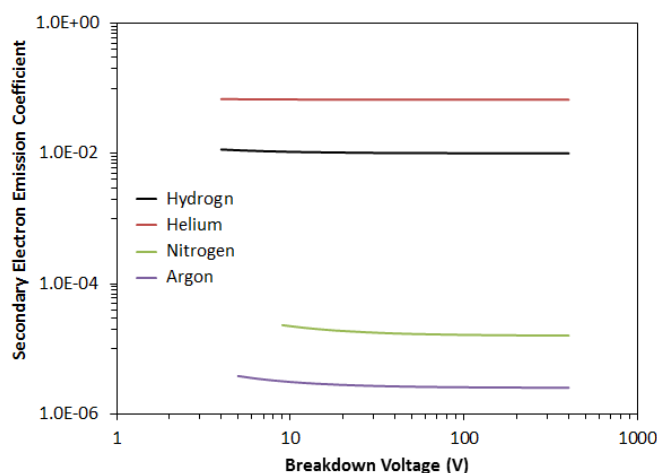

Fig. (5) Variation of secondary electron emission coefficient with breakdown voltage of four different gases at pressure of 0.1 mtorr and inter-electrode distance of 4 cm

Figure (7) shows the variation of secondary electron emission coefficient of cathode material with gas pressure of four different gases at breakdown voltage of 200 V and inter-electrode distance of 4 cm. it is clear that all gases are similar at very low gas pressures. However, high gas pressures make small differences in the values of emission coefficient, which means that the secondary electron emission is unavoidable at high pressures and other parameters can be considered to minimize the emission coefficient.

Figure (8) shows the variation of secondary electron emission coefficient of cathode material with inter-electrode distance for four different gases at pressure of 0.2 mtorr and breakdown voltage of

200V. Working at small inter-electrode distances submit an advantage of low emission coefficient of secondary electrons. Though, most applications require gas discharges at inter-electrode distances larger than 2 cm as the values of the minimum emission coefficient ranging from 100 to 1000. Larger distances would reduce the emission coefficient by more than an order of magnitude but higher voltages will be required for gas breakdown.
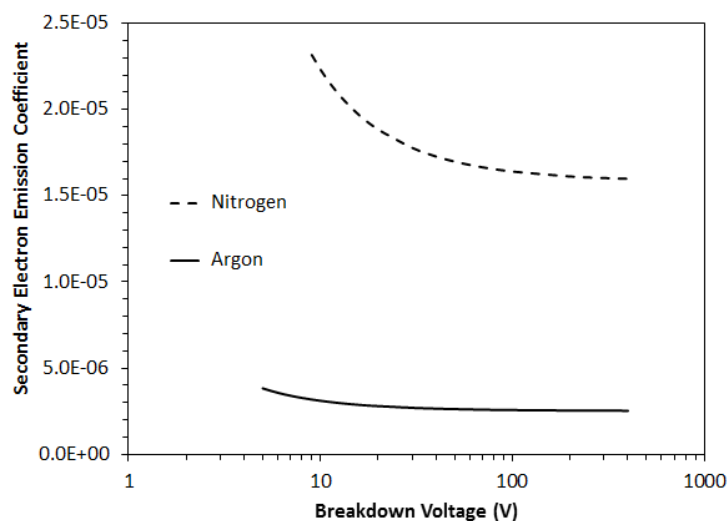

Fig. (6) Variation of secondary electron emission coefficient with breakdown voltage of four nitrogen and argon at pressure of 0.1 mtorr and inter-electrode distance of 4 cm
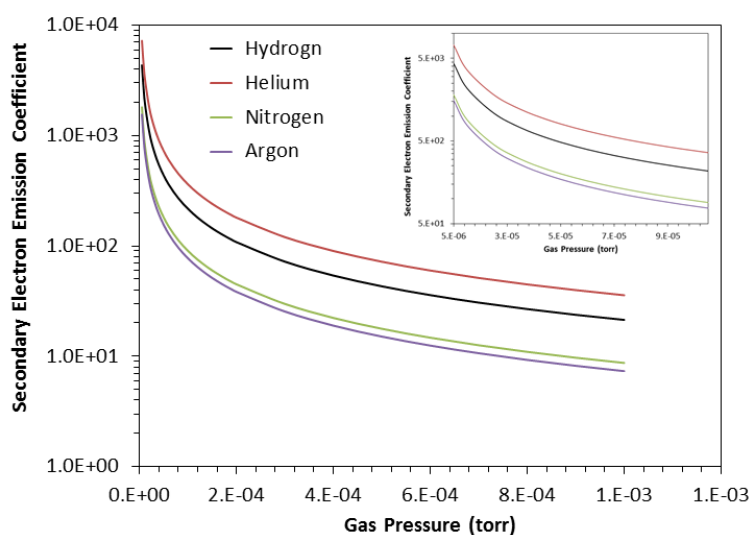

Fig. (7) Variation of secondary electron emission coefficient with gas pressure of four different gases at breakdown voltage of 200 V and inter-electrode distance of 4 cm
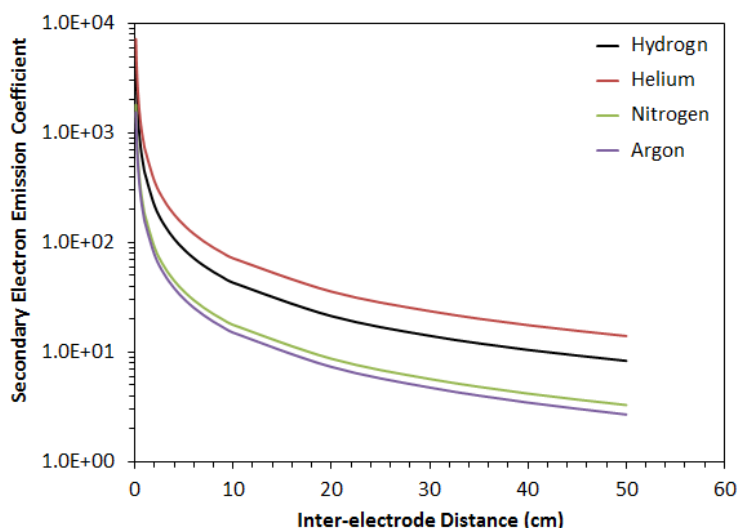
Fig. (8) Variation of secondary electron emission coefficient with inter-electrode distance for four different gases at pressure of 0.2 mtorr and breakdown voltage of 200 V

Helium is the most common gas in the practical uses of discharge plasmas, such as gas lasers and plasma processing. Therefore, it may be very advantageous to introduce the characteristics of secondary electron emission at experimental conditions (e.g., plasma sputtering). Figure (9) shows the variation of secondary electron emission coefficient of cathode material with gas pressure of helium at breakdown voltage of 190 V and inter-electrode distance of 4 cm. It is recommended to work at discharge gas pressures lower than 0.8 mtorr in order to keep the emission coefficient of secondary electrons lower than ten. Hence, the process employing discharge plasma can be performed with as much as possible investment of energy transferred to the discharge volume. This can be clearly observed in reactive sputtering processes as the electrical power remaining after the breakdown of discharge gas is mostly used for supporting the reaction of reactive gas with the sputtered atoms to form the required compound.
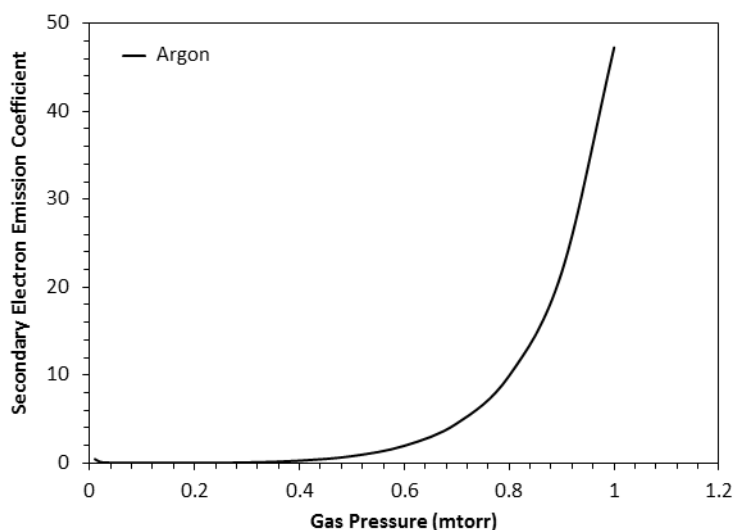

Fig. (9) Variation of secondary electron emission coefficient with gas pressure of helium at breakdown voltage of 190 V and inter-electrode distance of 4 cm

4. Conclusions

In concluding remarks, the emission coefficient of secondary electrons for some common gas discharges was determined as function of some affecting parameters. This coefficient has an important role in the optimization of discharge plasma employed for practical uses and applications. Therefore, this coefficient is often minimized even though the experimental conditions are shifted from

their optima in order to ensure that the consumption of supplied power is high as much as possible. This study was supported by experimental data from a reactive plasma sputtering system.

References

[1] M. Ohring, **"The Materials Science of Thin Films"**, Academic Press, p. 79, 112 (1992).

[2] D. Huy Trinh, Nanocrystalline Alumina-Zirconia Thin Films Grown by Magnetron Sputtering, Linköping University, Sweden, (2008) p. 1.

[3] K. Wasa, M. Kitabatake, H. Adachi, **"Thin Film Materials Technology: Sputtering of Compound Materials"**, William Andrew Inc., p. 139, 116, 2, 119, 72, 106, 103, 9 (2004).

[4] O.A. Hammadi, M.K. Khalaf and F.J. Kadhim, "Fabrication of UV Photodetector from Nickel Oxide Nanoparticles Deposited on Silicon Substrate by Closed-Field Unbalanced Dual Magnetron Sputtering Techniques", *Opt. Quantum Electron.*, 47(12), 3805-3813 (2015).

[5] O.A. Hammadi, M.K. Khalaf, F.J. Kadhim, "Fabrication and Characterization of UV Photodetectors Based on Silicon Nitride Nanostructures Prepared by Magnetron Sputtering", *Proc. IMechE, Part N, J. Nanoeng. Nanosys.*, 230(1) 32-36 (2016).

[6] O.A. Hammadi, M.K. Khalaf and F.J. Kadhim, "Silicon Nitride Nanostructures Prepared by Reactive Sputtering Using Closed-Field Unbalanced Dual Magnetrons", *Proc. IMechE, Part L, J. Mater.: Design and Applications*, 231(5), 479-487 (2017).

[7] D.R. Gibson, "Deposition of multilayer optical coatings using closed field magnetron sputtering", online article (2006).

[8] B.T. Chiad et al., "Characteristics and Operation Conditions of a Closed-Field Unbalanced Dual Magnetrons Plasma Sputtering System", *Open Access Library J.* (OALib), 1 (2014) e650. DOI:10.4236/oalib.1100650

[9] O.A. Hammadi and N.E. Naji, "Characterization of Polycrystalline Nickel Cobaltite Nanostructures Prepared by DC Plasma Magnetron Co-Sputtering for Gas Sensing Applications", *Photon. Sens.*, 8(1), 43-47 (2018).

[10] O.A. Hammadi, F.J. Al-Maliki and E.A. Al-Oubidy, "Photocatalytic Activity of Nitrogen-Doped Titanium Dioxide Nanostructures Synthesized by DC Reactive Magnetron Sputtering Technique", *Nonl. Opt. Quant. Opt.*, 51(1/2), 67-78 (2019)

[11] O.A. Hammadi et al., "Key Mechanisms of Low-Pressure Glow Discharge in Magnetized Plasmas", *Iraqi J. Appl. Phys.*, 12(3) (2016) 3-12.

[12] O.A. Hammadi et al., "Employment of Magnetron to Enhance Langmuir Probe Characteristics of Argon Glow Discharge Plasma in Sputtering System", *Iraqi J. Appl. Phys.*, 12(4) (2016) 19-28.

[13] M.A. Lieberman and A.J. Lichtenberg, **"Principles of Plasma Physics and Materials Processing"**, 2nd ed., Wiley (2005), p. 535, 547.

[14] M.K. Khalaf, O.A. Hammadi and F.J. Kadhim, "Current-Voltage Characteristics of DC Plasma Discharges Employed in Sputtering Techniques", *Iraqi J. Appl. Phys.*, 12(3) (2016) 11-16.

[15] O.A. Hammadi et al., "Operation Characteristics of a Closed-Field Unbalanced Dual-Magnetrons Plasma Sputtering System", *Bulg. J. Phys.*, 41 (2014) 24-33.

[16] F.F. Chen, **"Introduction to Plasma Physics and Controlled Fusion"**, 2nd ed., Plenum Press (NY, 1974), p. 22.

[17] C. O'Leary, Design, Construction and Characterisation of a Variable Balance Magnetron Sputtering System, Dublin City University, Ireland, p. 15 (1999).

[18] R.A. Swady, Development of vacuum technologies for the preparation of high-purity thin films in simple systems, PhD thesis, Loughborough University of Technology (1992), pp. 4-7, 19-21.

[19] T.J. Boyd and J. Sanderson, **"Physics of Plasmas"**, Cambridge University Press (2003).

[20] H.B. Nie, Thin Film Deposition and Characterization, National University of Singapore (NUS) (2014).

[21] B. Shah, Deposition of Tantalum on Steel by Sputtering, MSc thesis, New Jersey Institute of Technology (2001), p. 3, 15, 30.

[22] M. Julfikar Haider, Deposition of Hard and Solid Lubricant (TiN+MoS$_x$) Coating by Closed-Field Magnetron Sputtering, PhD thesis, Dublin University, Ireland (2005), pp. 56-58, 176.

[23] B.T. Chiad et al., "Langmuir Probe Diagnostics of Low-Pressure Glow Discharge Plasma Using Argon-Nitrogen Mixtures", *Iraqi J. Appl. Phys.*, 12(3) (2016) 17-26.

[24] O.A. Hammadi et al., "Magnetic Field Distribution of Closed-Field Unbalanced Dual Magnetrons Employed in Plasma Sputtering Systems", *Iraqi J. Appl. Phys.*, 12(3) (2016) 34-42.

[25] T. Tavsanoglu, Deposition and characterization of single and multilayered BC and BCN thin films by different sputtering configurations, PhD thesis, Université Technique d'Istanbul, Ecole des Mines de Paris (2009), p. 2, 16-23, 29.

[26] M.B. Hendricks et al., "Effects of ion-induced electron emission on magnetron plasma instabilities", *J. Vac. Sci. Technol.*, A12(4) (1994) 1408-1416.

[27] P.M. Martin, **"Introduction to Surface Engineering and Functionally Engineered Materials"**, John Wiley & Sons, Inc. (2011), p. 339.

[28] F. Ghaleb and A. Belasri, "Numerical and theoretical calculation of breakdown voltage in the electrical discharge", Radiation Effects and Defects in Solids, 1 (2012) 1-7.